Geosciences Journal
Vol. 11, No. 1, p. 59 − 73, March 2007

Monitoring of urban land surface subsidence using PSInSAR

Jun-su Kim — *School of Earth and Environmental Sciences (SEES), Seoul National University, Seoul 151-747, Korea*
Duk-Jin Kim — *Department of Naval Architecture and Marine Engineering, University of Michigan, Ann Arbor, Michigan, USA*
Sang-Wan Kim — *Rosenstiel School of Marine and Atmospheric Science, University of Miami, Miami, FL 33149, USA*
Now with Department of Geoinformation Engineering, Sejong University, Seoul 143-747, Korea
Joong-Sun Won — *Department of Earth System Sciences, Yonsei University, Seoul 120-749, Korea*
Wooil M. Moon* — *Geophysics, University of Manitoba, Winnipeg, MB, R3T 2N2, Canada*
Satellite Research Center, Research Institute of Oceanography, Seoul National University, Seoul 151-742, Korea

ABSTRACT: Space-borne and airborne SAR (Synthetic Aperture Radar) systems and SAR application technology have recently advanced greatly and interferometric SAR (InSAR) techniques can now be more effectively applied and used in many geological and engineering problems. There are several SAR data acquisition geometries for interferometric applications and PS (Permanent Scatter) InSAR (SAR interferometry) technique can accurately measure very small deformations on the Earth's surface with greatly increased precision. In this paper, the PSInSAR technique is tested and utilized to monitor and measure the land surface subsidence of areas near Incheon Port, and selected locations in Busan, Korea. All available JERS-1 (Japanese Earth Resource Satellite-1) L-band SAR data were acquired, processed and used to estimate the ground subsidence and subsidence rates, which range up to 30 mm/year.

Key words: InSAR, PSInSAR, land subsidence

I. INTRODUCTION

The performance of the well established differential InSAR (D-InSAR) technique is limited by decorrelation problem, in spite of the fact that the D-InSAR technique can detect terrain deformation up to a fraction of the microwave wavelength being employed. Interferometric SAR (Synthetic Aperture Radar) cannot easily be applied to the investigation of surface targets whose scattering characteristics change rapidly with time, such as rough water surface, melting or freezing snow covers, growing crop fields and forests, because of temporal decorrelation problems. Some of the well-known causes of geometric decorrelation are discussed by Zebker and Villasenor (1992). There have been numerous attempts to overcome these decorrelation problems in InSAR and D-InSAR computation, testing and utilizing spectral shifting (Gatelli et al., 1994), multiple baseline (Ferretti et al., 1996), radar polarimetry (Cloude and Papathanassiou, 1998), and permanent scatterer methods (Ferretti et al., 2000).

The PSInSAR is a newly developed surface displacement observation technique based on conventional radar interferometry (Ferretti et al., 2000). The PSInSAR technique was first proposed by Ferretti et al. (2000), and has been further developed and applied recently. Unlike earlier D-InSAR techniques, the PSInSAR requires as many interferometric data pairs as possible, at least 20 or more, for reliable final results. All available SAR images over the target study area are usually exploited, because the results from PSInSAR are more accurate when the greater the number of usable data pairs are available. In addition, the PSInSAR calculates instantaneously not only the motion of scatterers but also the propagation delay due to changes such as the atmosphere (e.g., APS; atmospheric phase screen) and the errors associated with the external DEM. Therefore, the possibility of misinterpretation owing to atmospheric factors and inaccuracies of the external DEM might be eliminated. While we can calculate more accurate results by removing undesirable components, ground deformation can be estimated only on some permanent scatterers, which do not change their scattering characteristics as a function of time or as a function of small changes of incident angle. The results are therefore sure to produce a sparse grid of displacements over a given study area. In spite of this restriction, a multi-dimensional interpolation scheme, such as Kriging, can give a desired estimation of deformation in regions of interest, since the deformation of the surface is strongly correlated in space and time.

D-InSAR and PSInSAR techniques have been applied to monitoring of surface displacements in various geological and related engineering problems (Massonnet and Feigl, 1998; Massonnet and Feigle, 1995; Moon et al., 1998; Massonnet et al., 1995; Raymond and Rudant, 1997; Write and Stow, 1999; Amelung et al., 1999; Sneed et al., 2001; Ferretti et al., 2001; Dehls et al., 2002; Declercq et al., 2005; Kim, 2007). In Earth science, various geological and geophysical processes cause surface deformation, including lateral movements and either surface subsidence or uplift. For instance, tectonic movement (Dehls et al., 2002)[1] tidal loading (Massonnet and Feigl, 1998)[1] volcanic activity (Massonnet et al., 1995), mine exploitation (Raymond and Rudant,

*Corresponding author: wmoon@eos1.snu.ac.kr

[1]Direct SAR application is not conducted but its physical feasibility was mentioned.

1997; Write and Stow, 1999), groundwater and oil withdrawal (Amelung et al., 1999; Sneed et al., 2001; Declercq et al, 2005), dissolution of soluble rocks such as halite (Baer et al., 2002), and unconsolidated basement (Kim et al., 2005) can trigger surface subsidence or inflation, while some others are accompanied by lateral displacements in such cases as earthquakes or glacial surges. Landslides often accompany both vertical and lateral movements. There have been many studies carried out to estimate the surface deformation from the above geological processes using InSAR technique. Some were successful and some were not (Massonnet and Feigl, 1998; Dehls et al., 2002). In Earth science, many geological processes related to vertical displacement can be characterized by their deformation behavior in terms of lateral, as well as vertical displacements and their deformation rates. Selected Earth's surface processes and the geological deformation processes are summarized in Table 1. (The references mentioned above are used as information sources.)

The accuracy of PSInSAR has been investigated in several studies (Colesanti et al., 2003; Dehls and Nordgulen, 2003). The study by Colesanti et al. (2003) monitored the fault creep along the Hayward Fault in California. In this case, Colesanti et al. (2003) estimated the line of sight (LOS) directional displacement rate due to fault creep using PSInSAR technique. The projection of LOS displacement along the fault direction was compared with creepmeter records with less than 10 percent error. Dehls and Nordgulen (2003) monitored land subsidence in Oslo in Norway caused by tunnel construction and related groundwater drainage. The subsidence of this study area was surveyed using leveling and the field records were compared to PSInSAR results. They were in good concordance, both in magnitude and in the short-term changes of deformation rate.

The PSInSAR technique has proved to be effective in many studies and is versatile to various surface deformation monitoring tasks. However, the limitations of PSInSAR technique should also be mentioned at this point. Firstly, PSInSAR technique cannot detect very rapid deformation because of aliasing. The critical deformation rate is half a wavelength per revisit period. In the case of JERS-1, the critical deformation rate is 12.5 cm in 44 days, or 2.7 mm in a day. Secondly, if a scatterer undergoes tilting related to ground deformation, it might change the scattering characteristics and it would not be detected as a PS (Permanent scatterer) (Dehls and Nordgulen, 2003). Lastly, PSInSAR cannot be applied to monitor the deformation of very large areas of which the length scale is larger than the swath of the image. This is because the InSAR techniques utilize the difference of phase relative to a stable point. If there is no stable point in the scene, the result will be biased as much as the deformation of the reference point.

In this study, we have investigated four study areas located in two different cities, in Korea – Incheon and Busan – and tried to estimate the degree of surface deformation. Highly populated urban environment restricts the detailed investigation of the geological causes of deformation including subsidence. Settling of unconsolidated basements (Kim et al., 2005), ground water withdrawal (Amelung et al, 1999; Declercq et al, 2005; Dehls and Nordgulen, 2003), and underground digging (Tesauro et al., 2000; Haynes et al., 1997) are possible causes. The Incheon study site is located at the west coast of the Korean Peninsula, along which a vast tidal flat is produced by high tidal amplitude. In Korea, a large portion of the reclaimed tidal flats are now converted into agricultural, industrial and residential areas. Approximately, one third of the urban area of Incheon is now built on such reclaimed lands and has potential problems of land subsidence. The other study sites in Busan are located at the south eastern tip of Korean Peninsula. The Nakdong River transports and deposits enormous amounts of fine sediments in the river mouth near Busan, and the new urban area, developed along the long narrow plain, is built on alluvial deposits. The PSInSAR technique was applied to monitor surface deformation over these two study areas utilizing all available JERS-1 SAR data acquired over the life-time of the JERS-1 satellite. The surface deformation in the Coastal Harbor of Incheon Port, which was reclaimed in the early 70's, and at Juan Railway Station, located about 6 km inland, is investigated assuming a linear deformation model. The subsidence of the Busan study site was first studied by Kim (2003) using PSInSAR technique, but we have independently carried out the investigation using the PSInSAR technique with additionally available SAR data. We included the two specific areas in Busan, where subsidence were previously studied by Kim (2003) – Bum Bridge and Deokpo Station, for mutual verification of our studies.

Table 1. Examples of Earth's surface deformation: displacement and time ranges

Geological Processes	Range (km)	Vertical Deformation (cm)	Time (year)
Tectonic Motion	10^2~10^3	~10^0 per year	Long period deformation.
Volcanic Activity	10^1	~10^1	Hourly ~ 10^0
Mine Exploitation	10^0	~10^1	10^{-1}~10^2
Soluble Rocks	10^0	~10^1	10^{-1}~10^0
Unconsolidated Basement	10^0~10^2	~10^1 per year	10^0~
Groundwater or Oil Extraction	10^1	~10^2	10^{-1}~10^1

2. PSInSAR TECHNIQUE

The PSInSAR is quite different from the traditional InSAR (SAR interferometry) technique. If N+1 Single Look Complex (SLC) images are re-sampled to a common master image, one can make N interferograms. One can remove the influence of the Earth's curvature from orbit information and of topography using both orbit information and external DEM. Then, one can get a series of phases for each pixel. The phases of an interferogram are influenced by several factors, such as linear phase ramp, inaccuracy of external DEM, atmospheric phase screen, the displacement of scatterer, and speckle and decorrelation noise. One of the common errors encountered in interferogram computation is a linear phase ramp (LPR) caused by inaccurate orbit determination. Inaccurate orbit information usually results in a repeating additional phase cycle along the range direction. Such a phase cycle is also found along the azimuth direction, but this usually has a longer wavelength and is caused by inaccuracies in satellite attitude and incomplete parallel orbits. For a small area, these cyclic phase patterns are usually eliminated assuming a linear phase model. Another factor influencing phase is the inaccuracy of external DEM or DEM error. In order to compute the differential interferogram, one needs to remove the phase from the topography. Although the topographic phase has removed the influence of topography from the interferogram, inaccurate external DEM remains the input causing non-zero residual phases in the interferogram. Residual phase due to inaccurate external DEM is different from interferogram to interferogram because the normal baseline of SAR data acquisition geometry is different from interferogram pair to interferogram pair. The third phase-influencing factor comes from the movement of target scatterers during two data acquisition periods. This is what one has to figure out, if the scattering characteristics of the target scatterers can be assumed to be fixed during the data acquisition periods. The fourth influencing factor is atmospheric phase delay. The atmosphere has a certain amount of water vapor content and it delays the propagation of microwaves emitted from the SAR antenna (Zebker et al., 1997). SAR records the retarded phase, as if the microwave has traveled a longer path. This is dubbed atmospheric phase screen (APS) (Ferretti et al., 2000, Ferretti et al., 2001). Some InSAR applications over high-relief areas report that remaining phases are related to the topography of the scattering surface because of the stratification of the atmosphere (Zebker et al., 1997; Kim, 2003). In this study, however, the effect of the stratified atmosphere is not considered because the study areas are flat and the effect of the atmosphere would be removed afterwards in PSInSAR process. The Busan study site has considerably more relief, but most permanent scatterers are distributed mostly over flat areas. The last factors are temporal and geometrical decorrelation noise. Temporal decorrelation results from the change of scattering characteristics of targets as a function of time. Temporal decorrelation is commonly found over agricultural crops, forest or vegetated areas. Geometrical decorrelation is due to the change of scattering characteristics as a function of radar geometry. Severe changes of scattering characteristics lower coherence and InSAR application becomes difficult or even impossible. A detailed summary of error factors associated with interferogram generation is given in Gens and Genderen (1996).

In the text, the use of 'normal' and 'vertical' is distinguished, in which both terms have the meaning of perpendicular relationship. The use of 'normal' is restricted to the use of 'normal baseline' which is the perpendicular component of baseline with respect to 'line of sight' direction. The use of 'vertical' is always related to the direction perpendicular to the 'ground', including for example, vertical deformation rate and vertical distance to satellite.

One can write a matrix formula describing the phase values of selected points (Ferretti et al., 2000).

$$\mathbf{\Phi} = \mathbf{\Phi}_{phase\ ramp} + \mathbf{\Phi}_{DEM\,error} + \mathbf{\Phi}_{deformation} + \mathbf{E} \tag{1}$$

where $\mathbf{\Phi}$ is a N (number of interferograms) by M (number of permanent scatterers) matrix and Φ_{ij} represents the phase of the j^{th} permanent scatterer in the i^{th} differential interferogram. For small processing areas, $\mathbf{\Phi}_{\text{phase ramp}}$ can be represented as $\mathbf{\Phi}_{\text{phase ramp}} = \vec{a}\vec{1}^{T} + \vec{p}_{\xi}\vec{\xi}^{T} + \vec{p}_{\eta}\vec{\eta}^{T}$, where $\vec{a}$ is the mean phase, $\vec{p}_{\xi}$ and $\vec{p}_{\eta}$ are the phase gradients along the range and azimuth directions respectively, and $\vec{\xi}$ and $\vec{\eta}$ are range and azimuth coordinates of permanent scatterers. They represent the equations of plane for each element. In physical sense, a linear phase ramp is due not only to inaccurate orbit and attitude determinations but also to very low frequency water vapor distribution in the troposphere. Gradual increase or decrease of phase delay caused by long wavelength variation of water vapor contents has an identical effect to a linear phase ramp in the interferogram (Ferretti et al., 2001). The phase due to DEM error is determined from DEM error by a simple proportionality relationship. In the case of repeat pass interferometry, the relation is $\phi = \frac{4\pi Bh}{\lambda r \sin\theta}$, where B is the normal baseline—baseline component perpendicular to LOS, h is DEM error, λ is wavelength, r is distance from satellite to scattering target, θ is the incident angle, and ϕ is phase in the interferogram due to DEM error. Like many other geophysical problems, the deformation rate can be found using a model; one can select which deformation model would be engaged. In many cases, surface deformation can be simplified as a time constant deformation (Ferretti et al., 2001) or a sinusoidal periodic deformation (Kampes and Hanssen, 2004). Deformation can even be considered as a stochastic one, but not deterministic (Ferretti et al., 2000). The time constant deformation model, however, was used in this study for the sake of simplicity. For the linear deformation model, the phase difference due to the moving scatterers is

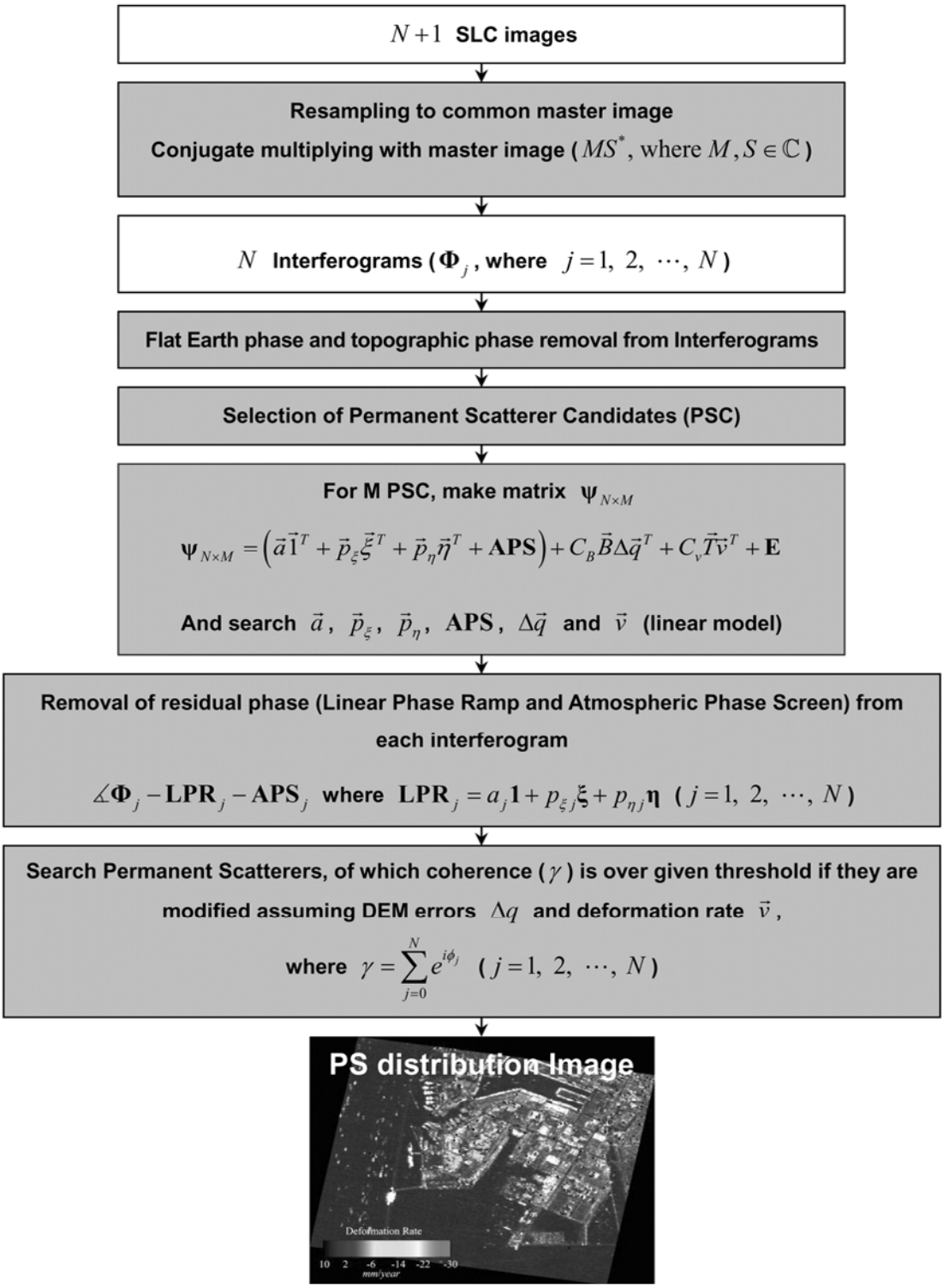

Fig. 1. Flow chart of PSInSAR technique.

calculated from $\phi = \frac{4\pi}{\lambda} Tv$ where T is a temporal baseline and v is the target velocity or deformation rate.

Because we know the normal baseline and temporal baseline of all interferogram pairs from the header file information, one can find the linear phase ramp, deformation rate and DEM error that will give the least error. This is a kind of over-determined problem because there are more known parameters (the normal baseline and temporal baseline of N

interferograms) than two unknown parameters (deformation rate and DEM error). What makes this problem more complex is that the phases are wrapped. Some different approaches to solve Equation with wrapped phase are given in Ferretti et al. (2001) and Kampes and Hanssen (2004). We made a two-dimensional model space of deformation rates and DEM error values, and calculated the ensemble phase coherence for each set of interferogram pairs in the model space in order to determine maximum coherence with the deformation rate and DEM error of that case. The ensemble phase coherence of j^{th} PS is defined as $\gamma_j = \left|\frac{1}{N}\sum_i^N e^{(\phi_i - C_q B_i \Delta q_j - C_v T_i v_j)}\right|$, which is the coherent sum of residual phases after deformation rate and DEM error are determined, or its amplitude in this context. The last term **E** in Equation 1 is the combination of the nonlinear atmospheric phase screen (APS) and decorrelation errors. Because the APS is highly related to spatial direction, one can separate the two contributions by a process of interpolation such as Kriging (Ferretti et al., 2000).

A flow chart for the PSInSAR technique is given in Figure 1. In order to calculate linear phase ramp (LPR) and APS, permanent scatterer candidate (PSC) is selected first. Pixels likely to be PS are selected as PSC, whose coherence is high and whose amplitude dispersion is not too big. Generally hundreds to thousands of PSCs are selected. LPR and APS are calculated from PSC. Because these two components have relatively little spatial variation, one can interpolate them into a uniform image grid, taking into account the power spectrum of APS (Williams et al., 1998). When these two components are removed from each interferogram, PS searching processing is followed in pixel by pixel basis. We may concern only two parameters, DEM error and deformation rate in this stage, because LPR and APS is already removed.

3. THE STUDY AREAS AND DATA SETS

The study areas investigated in this paper are located in two different cities, Incheon and Busan, but both situated in coastal areas of the Korean peninsula. These two cities include large reclaimed coastal areas, with probably large areas of unconsolidated ground material. The city of Incheon is located on the west coastline and Busan on the south eastern tip of the Korean Peninsula. Figure 2 shows geological maps of the two cities.

3.1. Incheon Study Area

The western coast of the Korean Peninsula is well known for its very high tidal amplitude. Gyeonggi Bay located approximately at the center of western coastline is one of the areas with tides reaching up to 9 meters. One of the world's largest tidal flats has developed along the shore of this bay. Incheon Port is located at the center of Gyeonggi Bay. To overcome a severe shortage of industrial space, a large portion of tidal flats have been reclaimed since the 1960's, and approximately one third of Incheon City is now built on reclaimed lands. (Fig. 2) A large portion of this reclaimed land is used for industrial and port supporting facilities, or simply as landfill sites. This study is conducted over the Coastal Harbor of Incheon Port and Juan Railway Station. The Coastal Harbor is built on reclaimed land, shaped as a small peninsula. It is used partly as a port, petroleum storage tanks, and partly as a residential area. Juan Railway Station is located about 6 km inland from the shore and surrounded by buildings standing on a granite basement. The railway runs in an east-west direction.

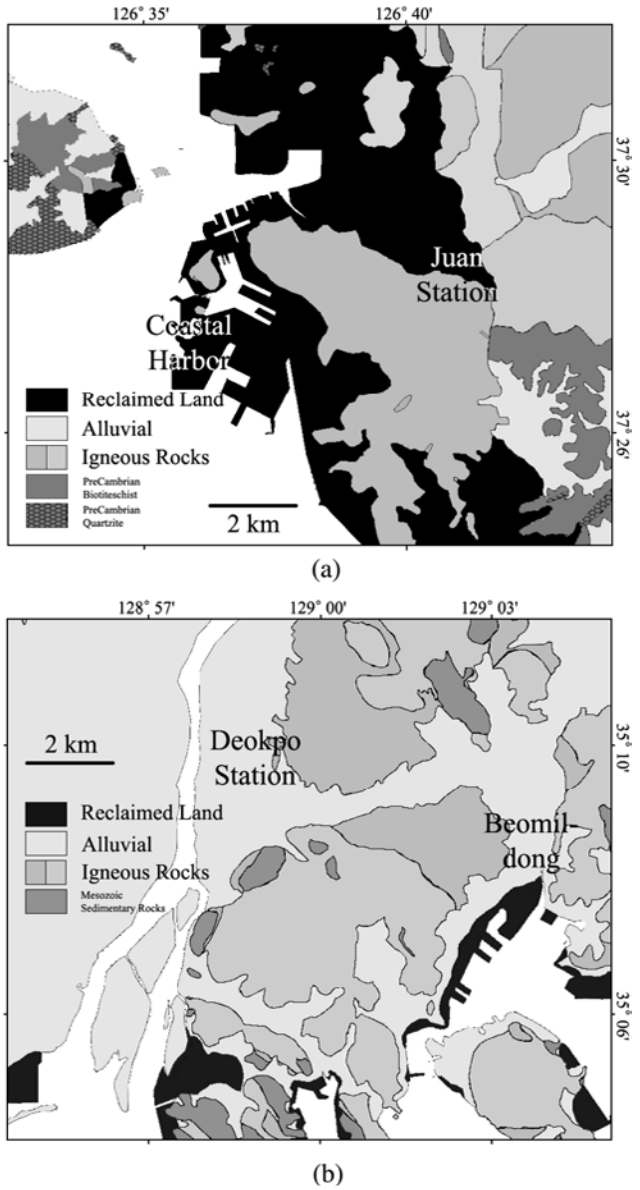

Fig. 2. The location and geological map of (a) Incheon and (b) Busan Study areas (Black area is reclaimed land).

3.2. Busan Study Area

The tidal amplitude of the south eastern coast of the Korean Peninsula is very small, at approximately 1 m or less, and relatively small tidal flats are developed in the vicinity of Busan City. Busan is not only one of the oldest commercial ports but also the second largest city in Korea. Various port facilities have been developed in Busan City over the last hundred years and almost every pier of Busan Port is built on some form of reclaimed land. Another geological factor that should be considered here is that, Nakdong River deposits large volumes of fine sediments on its mouth just behind Busan City. The delta areas of the Nakdong River mouth are used for various agricultural fields and industrial park developments, including the new airport facilities. Land subsidence events in the Busan area have previously been investigated by Kim (2003) using PSInSAR technique. There were two areas of noticeable subsidence; one is the Bum Bridge area and the other is the area around Deokpo Subway Station. In this study, four additional interferograms were added to the previous study (Kim, 2003) and the same PSInSAR processing was carried out as a way of verification of the result of Incheon Area.

4. SAR AND DEM DATA SETS

The L-band JERS-1 SAR data used include 27 scenes (row 89/path 238) over the Incheon area during the time period between 1992 and 1998. Detailed information on the SAR data is summarized in Table 2. The JERS-1 orbit was a near polar orbit and the orbit section was calculated from the CEOS header information as plotted in Figure 3a. The baseline diagram is plotted in Figure 3b. For Incheon, after reckoning in the normal baseline and temporal baseline, the scene acquired on Mar. 24, 1996 (#11) was set as the master scene and 26 interferograms were generated from SLC images. Unfortunately, only 23 interferograms were available in PSInSAR analysis because 3 SLC images (#4, #6, and #18) were acquired too far from the orbit tube, and produced very low-coherence interferograms. The PSInSAR technique has the potential to exploit the interferograms whose normal baselines are longer than the so-called critical baseline. For the three abandoned interferograms, however, we could not identify the linear fringe pattern due to orbit indeterminacy, and so these three interferograms were excluded. The rest of PSInSAR processing was carried out using 23 interferograms over the Coastal Harbor Peninsula

Table 2. Used JERS-1 SAR Data and orbit parameters (Incheon)

#	Date	Normal baseline (m)	Temporal baseline (years)	Coherence
1	1992/9/25	-2476.53	-3.493569	0.2509
2	1992/11/8	-490.98	-3.373101	0.3268
3	1992/12/22	-840.857	-3.252634	0.3124
4	1993/2/4	5621.158	-3.132166	Excluded
5	1993/3/20	29.55603	-3.011698	0.3148
6	1993/5/3	5904.169	-2.891230	Excluded
7	1993/6/16	1071.217	-2.770762	0.3013
8	1994/1/22	1914.88	-2.168422	0.2839
9	1994/8/30	-1397.78	-1.566083	0.3017
10	1995/2/22	-1235.21	-1.084211	0.3121
11	1996/3/24	Master	Master	Master
12	1996/5/7	1909.499	0.120468	0.3054
13	1996/6/20	848.1624	0.240936	0.3339
14	1996/8/3	1551.696	0.361404	0.3030
15	1996/12/13	2648.202	0.722807	0.2540
16	1997/1/26	2303.731	0.843275	0.2851
17	1997/4/24	2496.395	1.084211	0.2785
18	1997/7/21	-5182.69	1.325147	Excluded
19	1997/10/17	-2520.09	1.566083	0.2496
20	1997/11/30	-1675.56	1.686551	0.3009
21	1998/1/13	-714.489	1.807019	0.3319
22	1998/2/26	-2620.77	1.927487	0.2544
23	1998/4/11	-2051.04	2.047954	0.2594
24	1998/5/25	1653.179	2.168422	0.2921
25	1998/7/8	-1764.21	2.288890	0.2806
26	1998/8/21	-604.832	2.409358	0.3179
27	1998/10/4	-6.53814	2.529826	0.3118

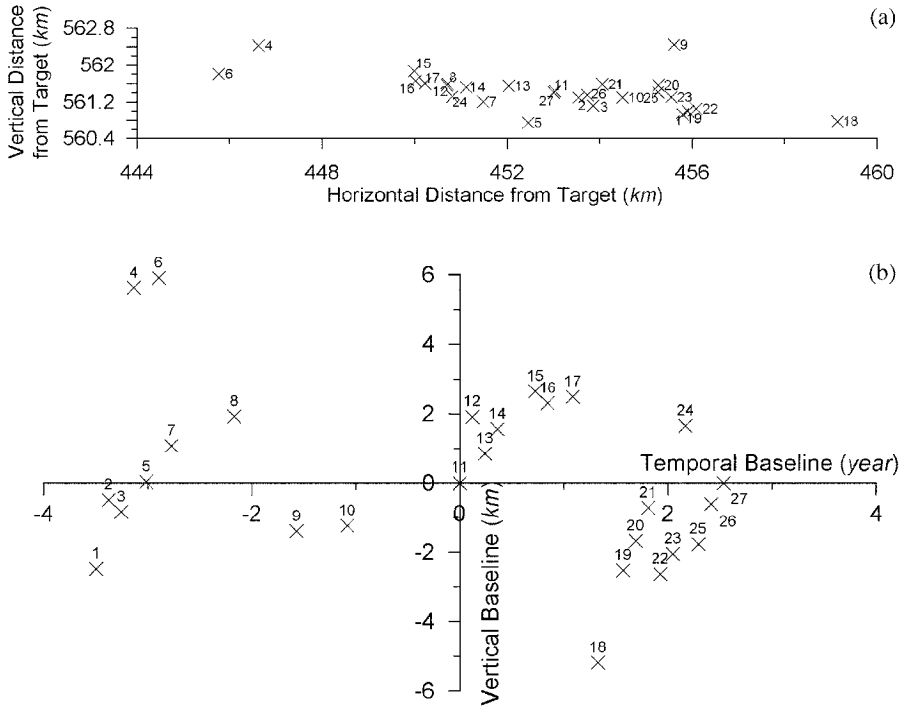

Fig. 3. The result of orbit analysis. (a) Orbit section diagram of JERS-1 SAR data and (b) Temporal normal baseline of SLC images over Incheon Study area. Numeric labels on each point are corresponding to the scene number given in Table 2.

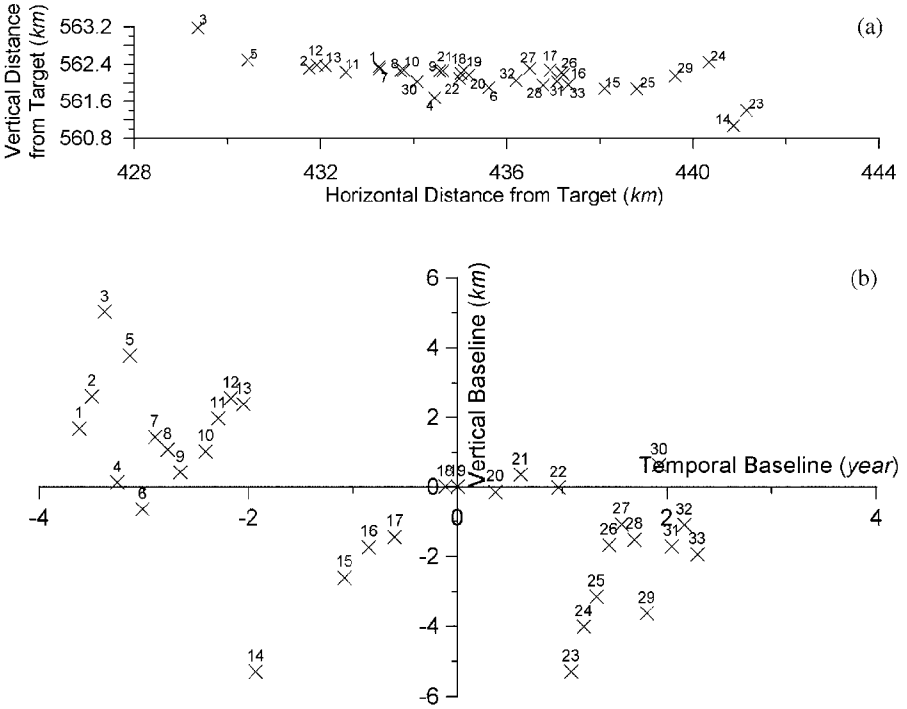

Fig. 4. The results of orbit analysis. (a) Orbit section diagram of JERS-1 SAR data and (b) Temporal normal baseline of SLC images over Busan Study area. Numeric labels on each point are corresponding to the scene number given in Table 3.

and Juan Railway Station in Incheon, assuming a linear deformation model.

For the Busan study area, 33 JERS-1 SAR scenes (row 83/path 242) were acquired during approximately the same period (Table 3). The scene acquired on Jun. 15, 1996 (#19) was set as the master scene and 26 interferograms were generated from SLC images and used in the PSInSAR analysis. According to Kim (2003), Bum Bridge and Deokpo Subway Station were the centers of local subsidence areas. These two area data were reprocessed and the results were analyzed in parallel with the previous results as a reference (Kim, 2003). The orbit section and baseline diagram of the Busan study area is given in Figure 4. A regional SAR image and highlighted study area maps of Incheon and Busan area are given in Figure 5a and b, respectively.

In this study, the public domain DEM from the NASA

Table 3. Used JERS-1 SAR Data and orbit parameters (Busan)

#	Date	Normal baseline (m)	Temporal baseline (years)	Coherence
1	1992/11/03	1672.97	-3.614037	0.4317
2	1992/12/17	2612.74	-3.493569	0.3593
3	1993/1/30	5028.47	-3.373101	Excluded
4	1993/3/15	128.469	-3.252634	0.5285
5	1993/4/28	3765.09	-3.132166	Excluded
6	1993/6/11	-648.337	-3.011698	0.5409
7	1993/7/25	1436.52	-2.891230	0.4451
8	1993/9/7	1070.34	-2.770762	0.4830
9	1993/10/21	414.17	-2.650294	0.5328
10	1994/1/17	1024.11	-2.409358	0.4811
11	1994/3/2	1967.44	-2.288890	0.4120
12	1994/4/15	2556.17	-2.168422	0.3610
13	1994/5/29	2383.20	-2.047954	0.3784
14	1994/7/12	-5288.40	-1.927487	Excluded
15	1995/5/16	-2605.36	-1.084211	0.3600
16	1995/8/12	-1734.58	-0.846275	0.4654
17	1995/11/8	-1443.15	-0.602340	0.4910
18	1996/5/2	2.76837	-0.120468	0.7441
19	1996/6/16	Master	Master	Master
20	1996/10/25	-149.642	0.361404	0.6488
21	1997/1/21	350.157	0.602340	0.6325
22	1997/6/2	-23.9296	0.963743	0.4927
23	1997/7/16	-5288.79	1.084211	Excluded
24	1997/8/29	-4008.50	1.204679	Excluded
25	1997/10/12	-3149.99	1.325147	0.3360
26	1997/11/25	-1677.79	1.445615	0.4080
27	1998/1/8	-1082.04	1.566083	0.4965
28	1998/2/21	-1525.36	1.686551	0.4507
29	1998/4/6	-3626.91	1.807019	Excluded
30	1998/5/20	632.746	1.927487	0.5689
31	1998/7/3	-1716.52	2.047954	0.4343
32	1998/8/16	-1099.24	2.168422	0.5023
33	1998/9/29	-1948.95	2.288890	0.3829

Shuttle Radar Topography Mission (SRTM) acquired in February 2000 was used as the external DEM. The U.S. Government has opened to the public the SRTM DEM with only a 3 arc second resolution, and its relative vertical accuracy is less then 10 meter (http://srtm.usgs.gov/Mission/quickfacts.html). The Coastal Harbor Peninsula is almost flat land, but SRTM DEM over this area shows significant effects of buildings and other facilities; the DEM value shows slight relief from 0 to 20 meter. This variation is apparently due to the influence over the area of buildings and is suppressed to be approximately 10 meter uniformly and the corrected SRTM DEM was used in the PSInSAR analysis of the Incheon study area. In the Busan study area, the original SRTM DEM was directly used without adjustment.

5. PSInSAR COMPUTATION RESULT

There are two areas of subsidence detected in the Incheon study area during the period of the JERS-1 SAR data acquisition between 1992 and 1998. The area with substantial subsidence is located in the Coastal Harbor Peninsula and another smaller area of subsidence is around the Juan Railway Station. In the Coastal Harbor area, the total area where PSInSAR technique was processed is approximately 5.25 km by 4.92 km and its land portion is 9.47 km^2, excluding the water covered areas. There were 3167 permanent scatterers (or PSs) detected when the ensemble phase coherence threshold was set to be 0.8, which corresponds approximately to 334 PSs per square kilometer. This number of PSs in the study area is moderate to dense compared to some

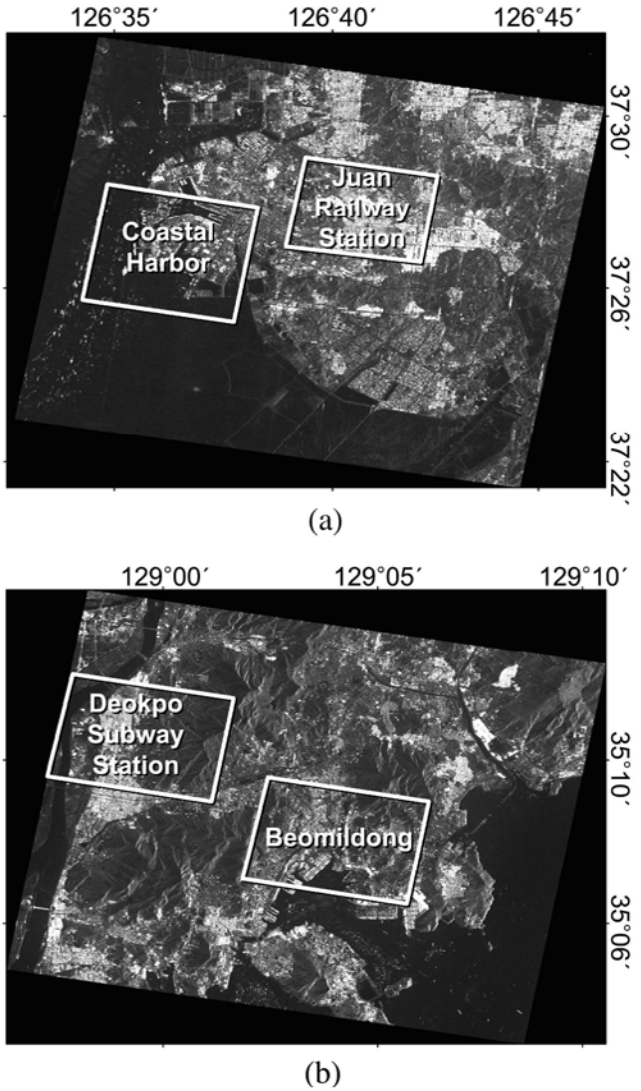

Fig. 5. Averaged backscattering intensity map of (a) Incheon and study area and (b) Busan study area.

other study areas observed with the same PSInSAR technique (Ferretti et al., 2000; Colesanti et al., 2003; Dehls and Nordgulen, 2003; Ferretti et al., 2001). The total area of investigation around Juan Railway Station is approximately 3.8 km by 4.6 km. Using the same coherence criteria, a total of 12183 PSs were detected, which is approximately 697 PSs per square kilometer, and this is a slightly greater PS density than the Coastal Harbor area. The area in the vicinity of Juan Railway Station is almost fully urbanized with very little vegetation cover.

The subsidence detected in the Coastal Harbor Peninsula area is significant (Fig. 6a). In the southern part of the Coastal Harbor Peninsula, there are petroleum storage facilities and an apartment complex next to each other. The shape of the subsided area is slightly elongated, but almost circular, and its diameter is approximately 2 km. The center of subsidence is observed in the middle part of the Coastal Harbor Peninsula and the subsidence rate was lower along the periphery of the peninsula. The maximum deformation rate is observed around the container yard located at the boundary between the apartment complex and the petroleum storage. The maximum deformation rate reached 3.0 cm/year in the line of sight (LOS) direction. Postulating that the displacement took place completely in a vertical direction, we should extract the vertical deformation rate by dividing its LOS component by the directional cosine of the incident angle. The nominal angle of incidence of the JERS-1 illumination geometry is 35 degrees and its cosine is 0.819. Small change of incident angle along range direction in swath results in a minor change of less than 4%. The estimated vertical deformation rate is 3.66 cm/year. The PS with high ensemble phase coherence (e.g., greater than 0.9), out of which the deformation rate is the maximum, was used as a reference point to decide the maximum deformation rate. Relatively little PSs are observed at the west of the maximum deformation (Figs. 6a and 7a). It is thought to be due to open fields with warehouses or the tilting of buildings caused by too much subsidence. While some parts of the reclaimed land areas suffered significant subsidence, the original natural land remained stable. For instance, Sowolmido Island situated just north of the Coastal Harbor Peninsular, separated by a narrow canal for ship passage, was originally a natural island that is now connected to the area of reclamation, whose basement rock is a Mesozoic igneous intrusion. Several buildings at the base of the island were detected as PS's and there was no sign of subsidence at all (Figs. 6a and Fig. 7d). Coal Pier, located along the southern side of the peninsula (Fig. 6a), also shows little sign of subsidence. It appears that Coal Pier was reclaimed later than the Coastal Harbor Peninsula area and the more recent constructions appear to be more stable than those of the main peninsular area (Fig. 6). In Figure 7, the deformation histories of other PSs in the Coastal Harbor are also shown.

Another area of subsidence is observed near Juan Railway Station and its vicinities (Fig. 6b). The subsidence rate estimated reaches approximately 15 mm/year in LOS. The shape of the area of subsidence is an ellipse elongated along the E-W direction. Its major axis is about one kilometer long. Its center is located slightly north of Juan Railway Station. Some PSs in this area exhibit a subsidence rate that varies with time (Fig. 8). They show a decreasing subsidence rate, which may mean that the area is slowly becoming settled. The greatest subsidence appears to have happened before 1995. It is, however, uncertain whether the subsidence of the Juan Railway Station area was really decreasing with time, since a time constant subsidence rate was assumed in this study. Some PSs showing typical time-varying deformation might be well excluded but some of them could be detected because the ensemble phase coherence threshold (0.8) gives a certain amount of tolerance. That means some linearly subsiding scatterers with specific phase noise were

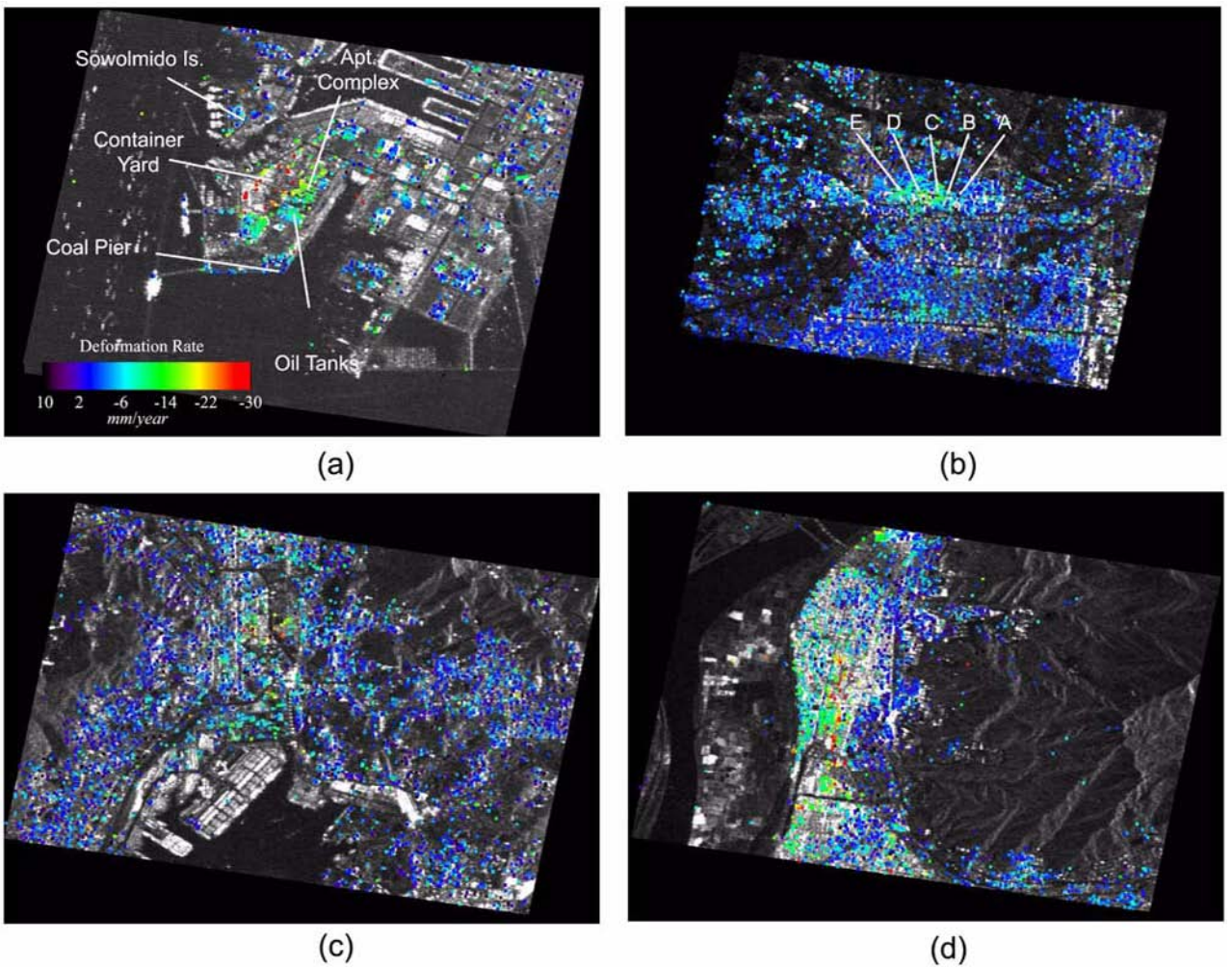

Fig. 6. Distribution of permanent scatters (PSs) in (a) Coastal Harbor area, (b) Juan Railway Station, in Incheon, (c) Beomildong, and (d) Deokpo Subway Station, in Busan. Yellow to red colored areas suffered subsidence. The deformation histories of indicated PS are represented in Figures 7 and 8, respectively.

detected as PSs with a decreasing subsidence rate on incidence. Figure 8 shows the deformation histories of five selected PSs of Juan Railway Station and its vicinity in spatial order. The decreases of the subsidence rate in both limbs are also noticeable.

In the Busan study area, the same two sub-areas of which subsidence were already discussed by Kim (2003) were analyzed. One is Beomildong and the other is Deokpo Subway Station. The distributions of PSs and their deformation rates are given in Figure 6c and d, respectively. Kim (2003) investigated the surface subsidence of the Busan area and indicated the subsidence of Bum Bridge and Deokpo Subway Station areas. The results in our study are compared with the previous study to cross-verify the results from Incheon. The Bum Bridge area in Kim (2003) is called Beomildong in this study because the term "Bum Bridge" represents only one structure rather than the whole area of investigation. According to Kim (2003), the deformation rate of the Beomildong area and that of Deokpo Subway Station are both approximately 2.5 centimeter per year. The averaged backscatter map of the Beomildong area, overlaid by the PS distribution map, is shown in Figure 6c. The maximum subsidence rate of the Beomildong area was 30 mm/year. This value is slightly higher than the value from the earlier study by Kim (2003). The deformation pattern is more complex in Deokpo Subway Station and its vicinity. The subsidence pattern is largely elongated in a direction almost parallel to the subway line but with a slight offset. The subsidence pattern is extended about 1.5 kilometers towards the north. The maximum subsidence is observed at the west of Deokpo Subway Station, which is located at the southern end of the linear subsidence area. The maximum deformation rate was 24 mm/year. One can conclude that the subsidence rate at Deokpo Subway Station is in good agreement with the earlier study (Kim, 2003).

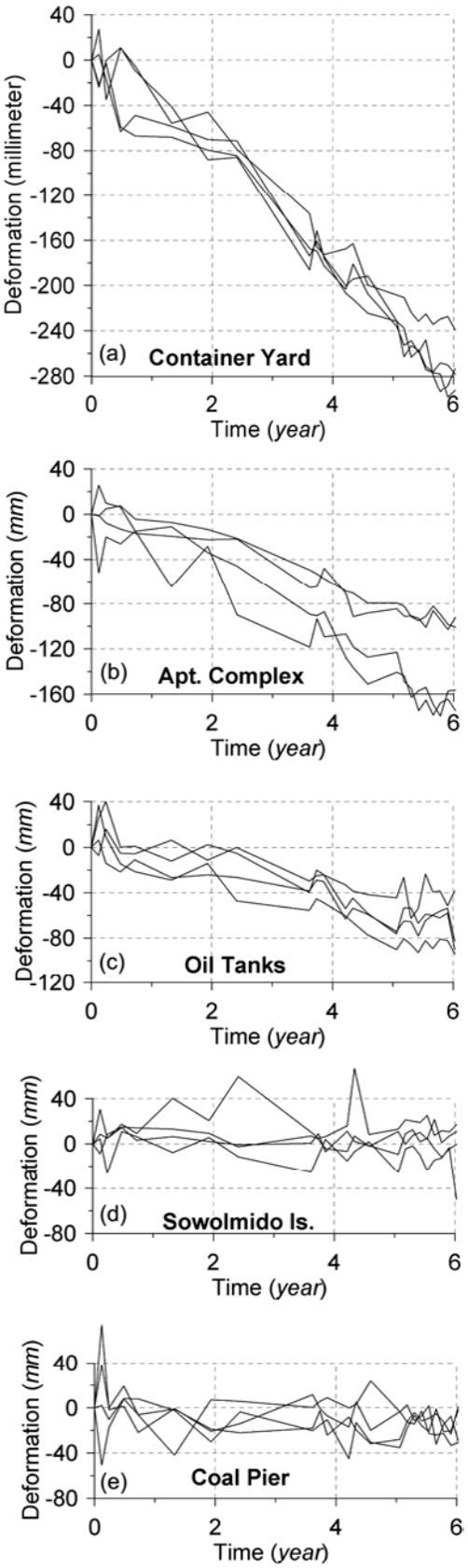

Fig. 7. The subsidence history of five sub-areas in Coastal Harbor study area.

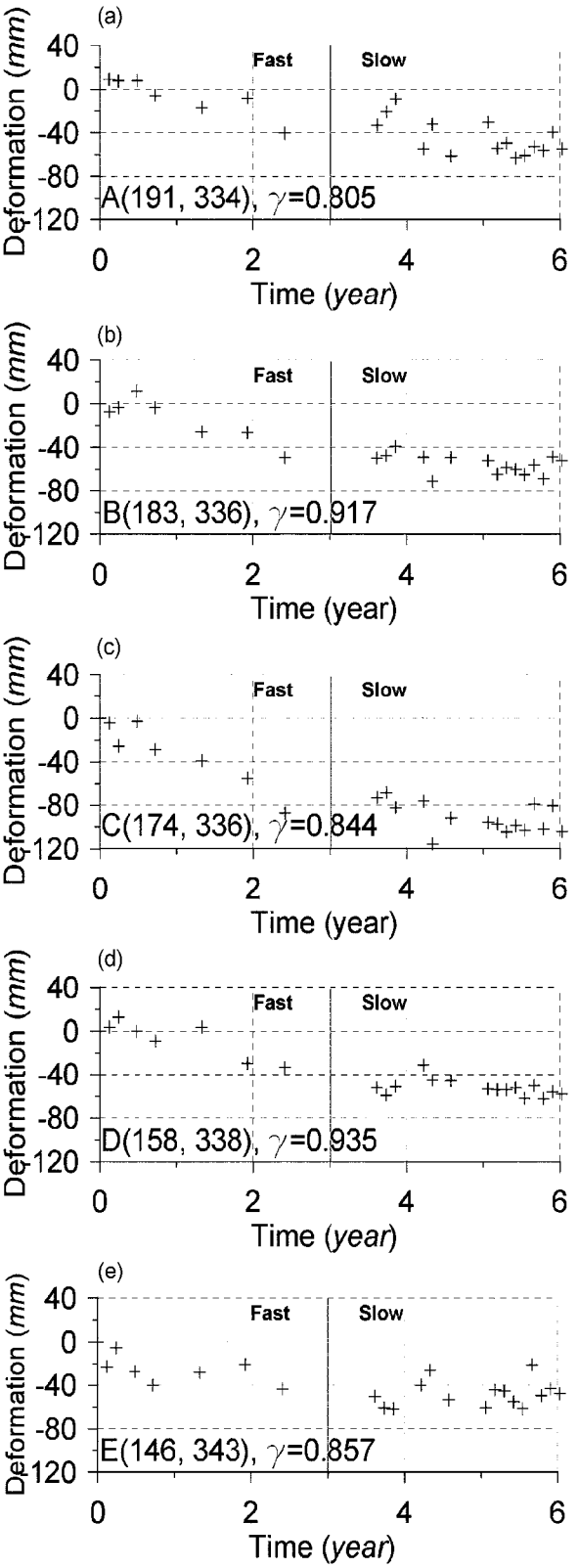

Fig. 8. Deformation history of PSs in Juan Railway Station area showing time varying deformation rate. Subsidence was observed during the first three years but deformation rate is declined during later three years. The spatial variation of subsidence rate is also presented. The time used in time axis begins on September 1992.

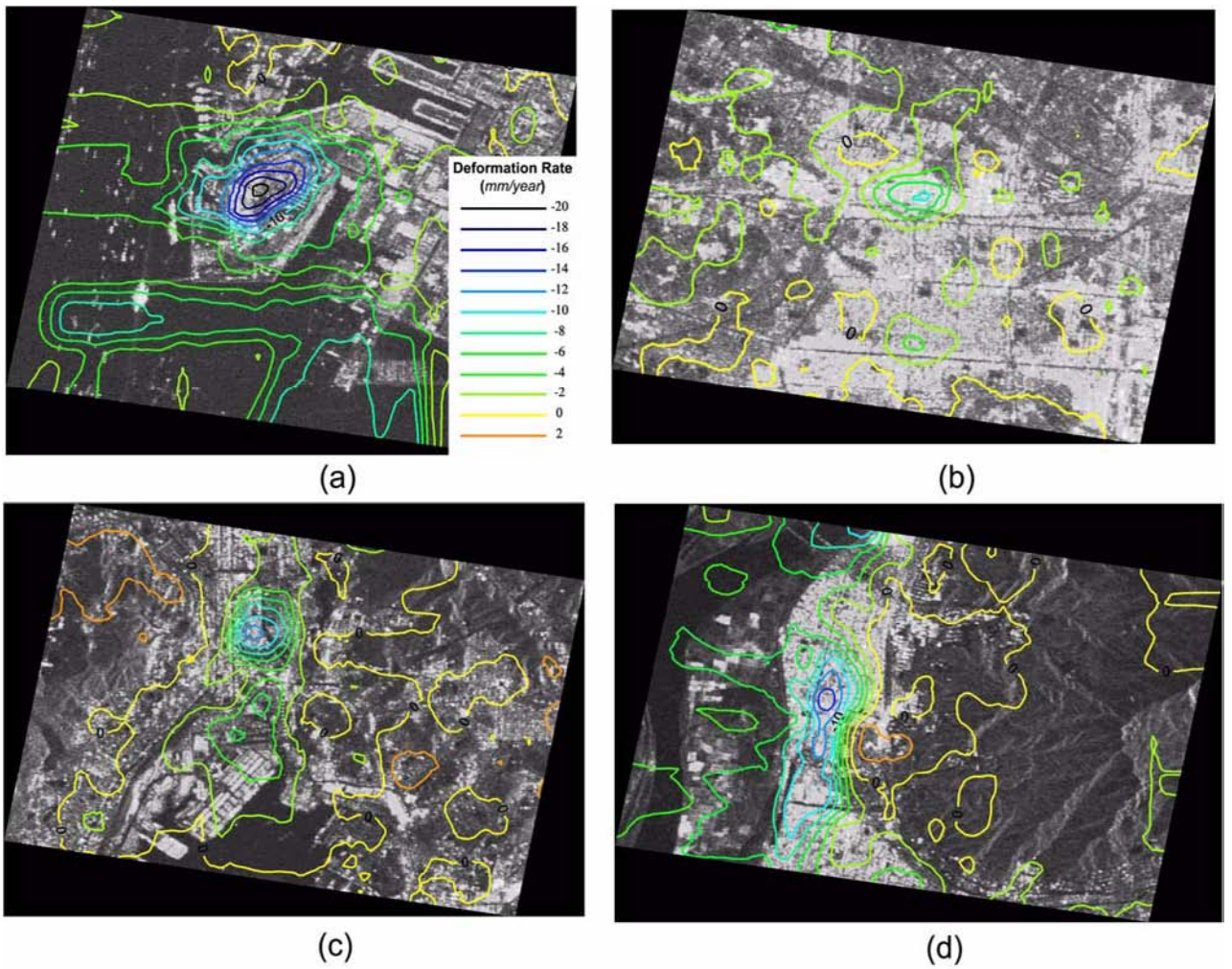

Fig. 9. The contour map of subsidence rate derived from kringing interpolation. Top left: Coastal Harbor, Top right: Juan Railway Station, Bottom left: Beomildong, and Bottom right: Deokpo Subway Station area. The deformation rate might have been slightly underestimated in general because of kriging interpolation and spatial filtering. In Coastal Harbor, contours over sea surface indicate spurious subsidence caused by sparse PS density and the nature of interpolation.

The deformation rate of PSs may not represent the deformation rate of the ground itself because many PSs are located off the ground, such as on a building or other structure. The response of each building varies slightly and results in a spatial dispersion of the deformation rate. In addition, when some non-stable target is identified as a PS by chance, it would not show spatial correlation with PSs nearby. We made a subsidence field map using Kriging interpolation to suppress the spatial variation (Fig. 9). The spatial distribution of the subsidence rate is clearly seen in these contour maps.

The accuracy of PSInSAR measurement of the Earth's surface displacements was assessed statistically in Colesanti et al. (2003). According to Colesanti et al., the standard deviation of phase residuals (σ_w) and the ensemble phase coherence of PSs (γ) can be related by the following equation:

$$\sigma_w \approx \sqrt{-2\ln|\gamma|} \tag{2}$$

Because the ensemble phase coherence threshold is set to be 0.8 in this study, the phase dispersion is 0.668 radians according to equation (2). The corresponding deviation of the displacement is calculated by multiplying by $4\pi/\lambda$, where λ is wavelength, and the result is 1.25 cm along LOS. The accuracy of DEM error and the deformation rate were also discussed in Colesanti et al. (2003) with the following relationships:

$$\sigma^2_{\text{DEM error}} = \frac{(\lambda r \sin\theta)^2 \sigma_w^2}{16\pi^2 \sum_{i=1}^{N} (B_i - \bar{B})^2}, \sigma_{\text{DEM error}} = \frac{\lambda r \sin\theta \sigma_w}{4\pi\sqrt{N}\sigma_B} \tag{3}$$

$$\sigma^2_{\text{deform rate}} = \frac{\lambda^2 \sigma_w^2}{16\pi^2 \sum_{i=1}^{N} (T_i - \bar{T})^2}, \sigma_{\text{deform rate}} = \frac{\lambda \sigma_w}{4\pi\sqrt{N}\sigma_T} \tag{4}$$

where $\sigma_{\text{DEM error}}$, $\sigma_{\text{deform rate}}$, σ_B, and σ_T are the standard deviation of the estimated DEM error, estimated deformation

rate, normal baseline, and temporal baseline, respectively, r is the distance between target and satellite, θ is the incident angle, B_i and T_i are the i^{ith} normal baseline and temporal baseline of the interferogram, respectively, and N is the number of scenes used.

Equation (3) assumes that the distribution of the normal baseline follows a normal distribution, and equation (4) assumes a regular acquisition time interval. The data acquisition criteria do not meet in these cases, but Equation (3) and (4) is applicable assuming the irregularity of data acquisition interval and normal baseline distribution do not produce big change. Calculated $\sigma_{\text{DEM error}}$ is 64 cm and $\sigma_{\text{deform rate}}$ is 1.22 mm/year in the Incheon study area. For the Busan study area, $\sigma_{\text{DEM error}}$ is 64.2 cm and $\sigma_{\text{deform rate}}$ is 1.17 mm/year.

6. DISCUSSION

The subsidence rates of four study sites in Incheon and Busan study areas are calculated using the PSInSAR technique. Land subsidence over reclaimed land is clearly observed on the Coastal Harbor Peninsula and the reclaimed areas appear to be settling down. In the Deokpo Subway Station area, at first sight, the recent subsidence appears to be related to sub-terrain digging associated with the new subway construction. However the subway was constructed in a slightly different position, offset by about one hundred meters. The causes of subsidence for the other two study sites are not clear at this time, but the investigation of the causes of subsidence is beyond the scope of this study.

The Coastal Harbor Peninsula was reclaimed more than 20 years before when JERS-1 was operational. Generally, the deformation should be waning with time after reclamation is completed and the high deformation rate (up to 3.7 cm/year) was an unexpected result. This anomalous phenomenon may have been caused by several factors: continuous reclamation of adjacent areas, sand-dominant reclamation material and subterranean structures such as oil storage tanks, and so on. The causes of subsidence over a long period of time in the study area have still to be investigated by geological engineers. The Juan Railway Station study site also showed significant surface deformation but its magnitude and deformation rate are not as large as those of the Coastal Harbor area. The major axis of Juan Railway Station's subsidence is well aligned with urban structures while its minor axis is relatively short. In addition, similar but weaker deformation signatures are found along another avenue of the south. So it is thought that the subsidence of Juan Railway Station and its vicinity is related to human activity but the reasons are again uncertain.

The subsidence of Busan study areas was already investigated using the PSInSAR technique. (Kim, 2003) In this study, we have estimated the subsidence using the same approach and with the same JERS-1 SAR data but with additional scene data. The resulting subsidence and subsidence rate are compared with the earlier study Kim (2003) and the subsidence rates at both sites are in good agreement with the results of earlier study. The subsidence of Deokpo Subway Station appears to be clearly related to recent subway construction, based on the facts that the area of subsidence is linear in shape and that the NS-directional major axis is nearly parallel to the subway line direction. However the reason for the offset between the subsidence and the subway line is unclear at this point. In the Sasang area, where Deokpo Subwauy Station is located, the sedimentary deposits are very thick because of the Nakdong River delta formation. The subsidence also appears to be extended towards the Nakdong River (Fig. 9d). The subsidence of the Beomildong site cannot be explained at this time and remains a mystery. This area is made of quaternary alluvial deposits but there is no clear geological explanation for abnormal subsidence relative to the stable surrounding areas. The perimeter of the subsidence in this site is well-rounded in shape. (Fig. 9c) Judging from Table 1, the most probable reason is ground water withdrawal. More careful scrutiny is required because large development projects are planned in the area.

7. CONCLUSIONING REMARKS

In this paper, the subsidence of urban areas was investigated with the PSInSAR technique utilizing the JERS-1 SAR data and the results were presented. This study has revealed that some parts of Incheon and Busan have been experiencing significant land subsidence during the 90's and seems to have continued until recently. The subsidence rate was approximately 30 mm/year in the Coastal Harbor of Incheon and 15 mm/year in the Juan Railway Station area. In the Busan area, the subsidence of the Beomildong area reached 30 mm/year and that of Deokpo Subway Station reached 24 mm/year. The precision of PSInSAR technique depends on the residual phase. The computational precision of PSInSAR technique using about two dozens of JERS-1 SAR data gives an accuracy of deformation rate approximately 1 mm/year when an ensemble phase coherence threshold is 0.8.

The land subsidence monitoring is often an important task for civil protection problems. The reclaimed coastal urban area is especially vulnerable to subsidence, not only because of its unconsolidated basement and groundwater exploitation but also because of a rapid sea level rise, possibly associated with current global warming. Conventional subsidence monitoring methods such as surveying and leveling require expensive maintenance and manpower costs. As a result, there have been little ground truth measurements over many cities in Korea. The PSInSAR technique can be applied to monitor these kinds of problem with far less cost. New approaches to monitoring land subsidence using satellite radar imagery (e.g., PSInSAR) are fully attributable to the

increasing archive of radar images. The PSInSAR technique successfully measured the subsidence of the coastal area quantitatively in the areas we have investigated.

However, the PSInSAR technique is not suitable for monitoring abrupt deformations faster than approximately half a wavelength scale per revisit time, approximately 1 m/year, in the case of the L-band JERS-1 SAR system. The tilting or rotation of buildings, or other permanent structures, associated with subsidence can result in the changes of scattering characteristics and these types of PS will be lost. This kind of situation will be an unfortunate practical obstacle in the application of PSInSAR. Large areas of subsidence, such as those observed in many tectonic problems, which are wider than image swaths, cannot be monitored using PSInSAR technique alone. We will then need a network of reference GPS stations in the target area. The PSInSAR technique is a particularly good way to monitor land subsidence in urban areas, even though there are still many minor technical problems to solve.

ACKNOWLEDGMENT: This work is funded by Korean Meteorological Administration (KMA) Research and Development Program under grant CATER 2006-5203. The satellite JERS-1 data used in this study were made available by the grants by the Electronic and Telecommunication Research Institute (ETRI), the NSERC of Canada Discovery Grant (A-7400), and Do-Wha Research Grant to W.M. Moon. The authors would like to thank colleague Sang-Eun Park in the ESI^3 Laboratory at the Seoul National University.

REFERENCE

Amelung, F., Galloway, D.L., Bell, J.W., Zebker, H.A. and Laczniak, R.J., 1999, Sensing the ups and downs of Las Vegas: InSAR reveals structural control of land subsidence and aquifer-system deformation, Geology, 27, 483–486.

Baer, G., Schattner, U., Wachs, D., Sandwell, D., Wdowinski, S. and Frydman, S., 2002, The lowest place on Earth is subsiding-An InSAR (interferometric synthetic aperture radar) perspective, Geological Society of America Bulletin, 114, 12–23.

Cloude, S.R. and Papathanassiou, K.P., 1998, Polarimetric SAR interferometry, IEEE Transaction on Geoscience and Remote Sensing, 36, 1551–1565.

Colesanti, C., Ferretti, A., Novali, F., Prati, C. and Rocca, F., 2003, SAR monitoring of progressive and seasonal ground Deformation using the permanent scatterers technique, IEEE Transaction on Geoscience and Remote Sensing, 41, 1685–1701.

Declercq, P-Y., Devleeschouwer, X. and Pouriel, F., 2005, Subsidence revealed by PSInSAR technique in the Ottignies-Wavre area (Belgium) related to water pumping in urban area, 4th Fringe Workshop (Expanded Abstract), Frascati, Nov. 28–Dec. 1.

Dehls, J.F., Basilico, M. and Colesanti, C., 2002, Ground deformation monitoring in the Ranafjord area of Norway by means of the permanent scatterers technique, 23th International Geoscience and Remote Sensing Symposium (Expanded Abstract), Toronto, June 24-28, p. 203–207.

Dehls, J. and Nordgulen, Ø., 2003, Analysis of InSAR data over Romeriksporten, 2003.076, Geological Survey of Norway, 18 p.

Ferretti, A., Guarniert, A.M., Prati, C. and Rocca, F., 1996, Multi-baseline interferometric techniques and applications, Fringe Workshop (Expanded Abstract), Zurich, Sep. 30-Oct. 2.

Ferretti, A., Prati, C. and Rocca, F., 2000, Nonlinear subsidence rate estimation using permanent scatterers in differential SAR interferometry, IEEE Transaction on Geoscience and Remote Sensing, 38, 2202–2212.

Ferretti, A., Prati, C. and Rocca, F., 2001, Permanent scatterers in SAR interferometry, IEEE Transaction of Geoscience and Remote Sensing, 39, 8–20.

Gatelli, F., Guarnieri, A.M., Parizzi, F., Pasquali, P., Prati, C. and Rocca, F., 1994, The wavenumber shift in SAR interferometry, IEEE Transaction on Geoscience and Remote Sensing, 32, 855–865.

Gens, R., Van Genderen, J.L., 1996, SAR interferometry-issues, techniques, applications, International Journal of Remote Sensing, 17, 1803–1835.

Haynes, M., Capes, R., Lawrence, G., Shilston, D. and Nicholls, D., 1997, Major urban subsidence mapped by differential SAR interferometry, 3rd ERS Symposium on space at the service of our Environment (Expanded Abstract), Florence, Mar. 17–20.

Kampes, B. and Hanssen, R., 2004, Ambiguity resolution for permanent scatterer interferometry, IEEE Transaction Geoscience and Remote Sensing, 42, 2446–2453.

Kim, S.W, 2003, Measurement of surface displacement of Mt. Baekdu and Busan area using L-band SAR interferometry, Ph. D. Thesis, Yonsei University, 157 p. (In Korean with English abstract)

Kim, S.W, Ferretti, A., Novali, F., Wdowinski, S., Amelung, F., Dixon, T.H., Dokka, R.K. and Rabus, B., 2005, Observation of subsidence in New Orleans using permanent scatterers, 2005 Joint Assembly [AGU, SEG, NABS and SPD/AAS] (Abstract), New Orleans, May 25-27, G43A-04.

Kim, J., 2007, Monitoring of surface deformation in urban areas using PSInSAR technique, M. Sc. Thesis, Seoul National University, 109 p.

Massonnet, D., Feigle, K.L., 1995, Satellite radar interferometric map of the coseismic deformation field of the M = 6.1 Eureka Valley, California earthquake of May 17, 1993, Geophysical Research Letters, 22, 1541–1544.

Massonnet, D., Briole, P. and Arnaud, A., 1995, Deflation of Mount Etna monitored by spaceborne radar interferometry, Nature, 375, 567–570.

Massonnet, D. and Feigl, K.L., 1998, Radar interferometry and its application to changes in the Earth's surface, Reviews of Geophysics, 36, 441–500.

Moon, W.M., Ristau, J., Vachon, P., 1998, Feasibility of applying apace-borne SAR interferometry for earthquake tectonic investigation, Geoscience Journal, 2, 78–87.

Raymond, D. and Rudant, J.P., 1997, ERS-1 SAR Interferometry: Potential and limits for mining subsidence detection, 3rd ERS Symposium on Space at the Service of Our Environment (Expanded Abstract), Florence, Mar. 17-20, p. 541–544.

Sneed, M., Ikehara, M., Balloway, D.L. and Amelung, F., 2001, Detection and measurement of land subsidence using global positioning system and interferometric synthetic aperture radar, Coachella Valley, California 1996-1998, Water-Resources Investigations Report, 01-4193, US Geological Survey.

Tesauro, M., Bererdino, P., Sansosti, E., Fomaro, G. and Franseschetti, G., 2000, Urban subsidence inside the city of Napoli (Italy) observed by satellite radar interferometry, Geophysical Research Letters, 27, 1961–1964.

Williams, S., Bock, Y. and Fang, P., 1998, Integrated satellite inter-

ferometry: Tropospheric noise, GPS estimates and implications for interferometric synthetic aperture radar products, Journal of Geophysical Research, 103, 27051–27067.

Write, P. and Stow, R., 1999, Detecting mining subsidence form space, International Journal of Remote Sensing, 20, 1183–1188.

Zebker, H. A. and Villasenor, J., 1992, Decorrelation in interferometric radar echoes, IEEE Transaction on Geoscience and Remote Sensing, 30, 950–959.

Zebker, H. A., Rosen, P. and Hensley, S., 1997, Atmospheric effects in interferometric synthetic aperture radar surface deformation and topographic maps, Journal of Geophysical Research, 102, 7547–7563.

Manuscript received August 26, 2006
Manuscript accepted March 21, 2007